

Electronic Supplementary Information for

Promoting defective-Li₂O₂ formation *via* Na doping for Li-O₂ batteries with low charge overpotentials

Zhiyang Lyu,^{†*ab} Tao Wang,^{†c} Rui Guo,^{†b} Yin Zhou,^b Junchao Chen,^d Xiao Wang,^d Ming Lin,^e XinXin Tian,^f Min Lai,^a Luming Peng,^d Li Wang,^g Zhangquan Peng,^h and Wei Chen^{*bij}

^aSchool of Physics and Optoelectronic Engineering, Nanjing University of Information Science & Technology, Nanjing 210044, Jiangsu, China

^bDepartment of Chemistry, National University of Singapore, 3 Science Drive 3, 117543, Singapore.

^cSUNCAT Center for Interface Science and Catalysis, Department of Chemical Engineering, Stanford University, Stanford, California 94305, USA.

^dKey Laboratory of Mesoscopic Chemistry of MOE, School of Chemistry and Chemical Engineering, Nanjing University, Nanjing 210023, China.

^eInstitute of Materials Research and Engineering, A*STAR (Agency for Science, Technology and Research), 2 Fusionopolis Way, Innovis, Singapore.

^fInstitute of Molecular Science, Key Laboratory of Materials for Energy Conversion and Storage of Shanxi Province, Shanxi University, Taiyuan 030006, China.

^gDepartment of Physics, Nanchang University, Nanchang, 330031, China.

^hState Key Laboratory of Electroanalytical Chemistry, Changchun Institute of Applied Chemistry, Chinese Academy of Science, Changchun, Jilin 130022, China

ⁱDepartment of Physics, National University of Singapore, 2 Science Drive 3, 117543, Singapore.

^jNational University of Singapore (Suzhou) Research Institute, Suzhou, 215123, China.

[†]These authors contributed equally to this work.

*E-mail: mselyuz@nus.edu.sg; phycw@nus.edu.sg;

Details of theoretical simulation

All computations were performed by applying the plane-wave based density functional theory (DFT) method with the Vienna Ab Initio Simulation Package (VASP).^{1,2} The electron ion interaction was described with the projector augmented wave (PAW) method,^{3,4} while the electron exchange and correlation energy was solved with the Heyd–Scuseria–Ernzerhof (HSE) screened hybrid functional.⁵ The screened exchange mixing parameter was set as 0.207, which was the same as the literature of the HSE06 functional.⁶ An energy cut-off of 400 eV and a second-order Methfessel-Paxton electron smearing with 0.2 eV were used to ensure accurate energies.⁷ Geometry optimization was done when forces became smaller than 0.02 eV/Å and the energy difference was lower than 10⁻⁵ eV. The calculated lattice parameters of hexagonal Li₂O₂ with a space group of P63/mmc are a = b = 3.100 Å, c = 7.516 Å, which are in good agreement with experimental values.⁸ The formation energy of Li_xNa_yO₁₆ are calculated by using different energy references:

(a): energy references are metallic bulk Li and Na

$$\text{Formation energy} = \frac{E(\text{Li}_x\text{Na}_y\text{O}_{16}) - xE(\text{Li}_{\text{bulk}}) - yE(\text{Na}_{\text{bulk}}) - 8 * E(\text{O}_2)}{N_{\text{atoms}}}$$

(b): energy references are Li₂O₂ and Na₂O₂

$$\text{Formation energy} = \frac{E(\text{Li}_x\text{Na}_y\text{O}_{16}) - xE(\text{Li}_2\text{O}_2)/2 - yE(\text{Na}_2\text{O}_2)/2 - (16 - x - y) * E(\text{O}_2)/2}{N_{\text{atoms}}}$$

(c): energy references are Li₂O₂ and NaO₂

$$\text{Formation energy} = \frac{E(\text{Li}_x\text{Na}_y\text{O}_{16}) - xE(\text{Li}_2\text{O}_2)/2 - yE(\text{NaO}_2)/2 - (16 - x - 2y) * E(\text{O}_2)}{N_{\text{atoms}}}$$

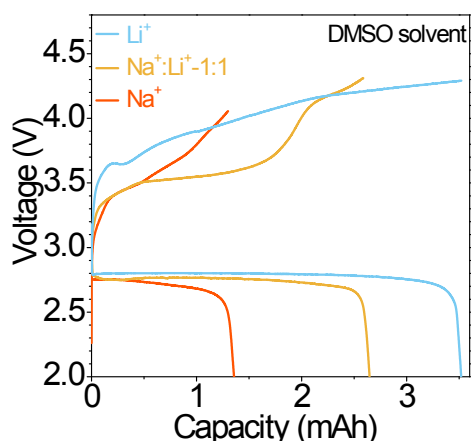


Figure S1. The full discharge-charge curves of the cells with different marked electrolytes at a current of 0.1 mA.

Even under full discharge-charge condition, Na^+ also plays a significant role in reducing charge overpotentials (Figure S1). The discharge capacities of the cells with the added Na^+ electrolytes are lower than that of the pure Li^+ electrolyte. This could originate from the fact that the cathode surfaces with the added Na^+ electrolytes are easy to be passivated by large-size discharge products (Figure S2). This is different from a previous case where the solution phase formation of discharge products were promoted by adding additives 2,5-di-tert-butyl-1,4-benzoquinone (DBBQ) in electrolyte.⁹ Thus the discharge capacity can be increased compared to that of the cell without added DBBQ (nearly 0 mAh cm^{-2}). However, the cathode surface still will to be passivated by large-size discharge products, leading to a sudden death. Moreover, the DBBQ additive operates a different mechanism that avoids the reactive LiO_2 intermediate in solution.

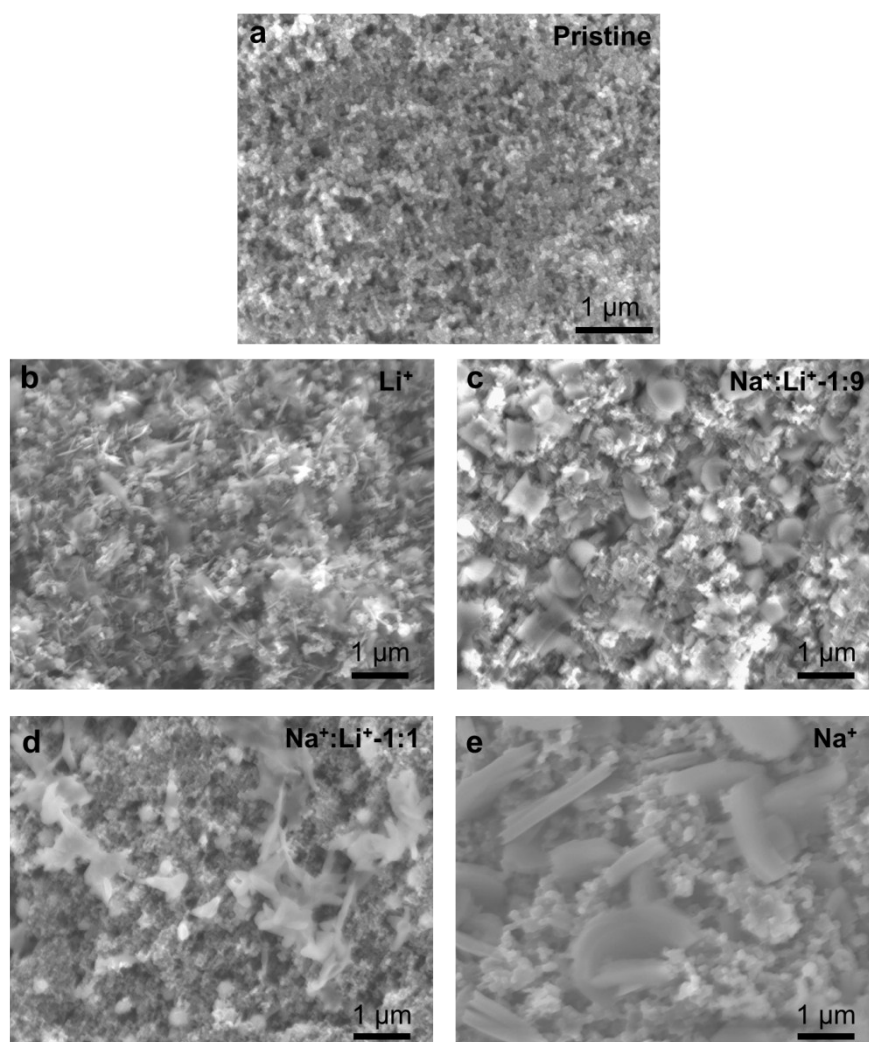


Figure S2. SEM images of the discharge product for the cells with different marked electrolytes at a limited capacity of 1 mAh and a current of 0.1 mA. **a**, Pristine. **b**, Li⁺. **c**, Na⁺:Li⁺-1:9. **d**, Na⁺:Li⁺-1:1. **e**, Na⁺.

With increasing added amount of Na⁺, the size of the discharge product increases, which could arise from insertion of higher amount of the large-radius Na⁺.

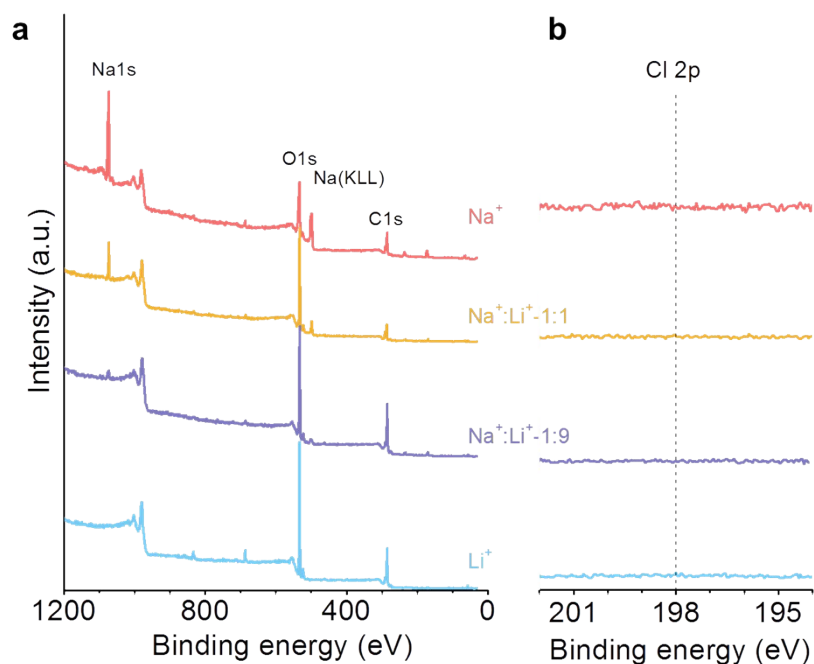


Figure S3. XPS characterizations of the discharge product for the cells with different marked electrolytes. **a**, XPS survey scan spectra. **b**, Spectra of Cl 2p.

As shown in Figure S3, the absence of Cl element in XPS result reveals that the added NaClO_4 salt is fully washed. This result indicates the Na signal arises from the discharge products, not from the NaClO_4 salt.

Table S1. The atomic concentrations (at%) from XPS for all samples

Sample	Li^+	$\text{Na}^+:\text{Li}^+-1:9$	$\text{Na}^+:\text{Li}^+-1:1$	Na^+
Na	—	2.09	3.85	5.60
Li	49.81	47.23	45.22	40.98
O	50.19	50.68	50.93	53.42

Note S1: The consideration for the structure of discharge product

Although the Na⁺ concentration of electrolyte is high (i.e., 0.5M), it seems that the discharge product is only NaO₂. When the added electrolyte is 50 μL, the corresponding discharge capacity is calculated to be 0.67 mAh, which is smaller than the limited value of 1 mAh. This confirms that the Li⁺ ions oxidized from lithium anode are inevitably involved in the discharge reaction. Moreover, the XPS data demonstrate that the Na content in discharge products is only 5.60 at% even for the 0.5M Na⁺ sample, revealing that the products are mainly Li₂O₂ structure not NaO₂ structure (Table S2). In addition, the nanosheet-like morphologies of products are quietly different from the typical cube morphology of NaO₂, also suggesting the formation of products with Li₂O₂ structure (Figure S2).



$$N_{\text{Na}^+} = 0.5 \text{ mol/L} \times 0.05 \times 10^{-3} \text{ L} \times 6.02 \times 10^{23} / \text{mol} = 1.505 \times 10^{19}$$

$$Q_{\text{NaO}_2} = N_{\text{Na}^+} \times e = 1.505 \times 10^{19} \times 1.6 \times 10^{-19} \text{ C} = 2.408 \text{ C} = 0.67 \text{ mAh}$$

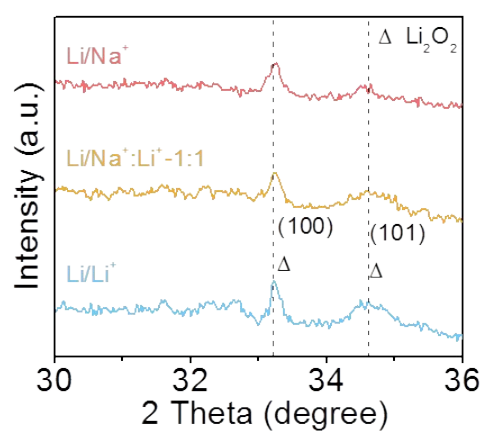


Figure S4. XRD patterns of the discharge products of the cells with different marked electrolytes.

The XRD peaks of the products with different Na doping are weaker and flat than that of pristine one, demonstrating the products became amorphous due to the induced defects.

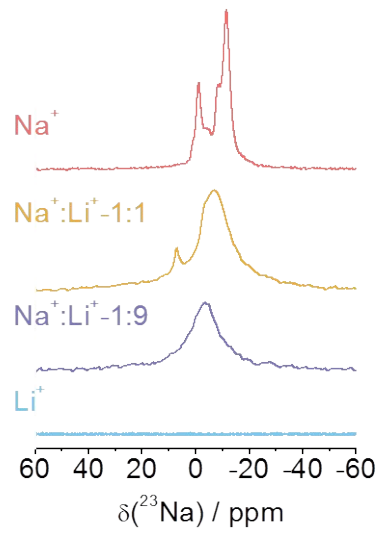


Figure S5. ^{23}Na ssNMR spectra of the discharge products for the cells with marked electrolytes.

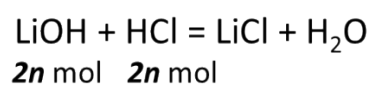
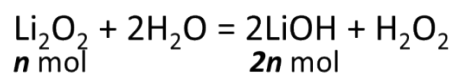
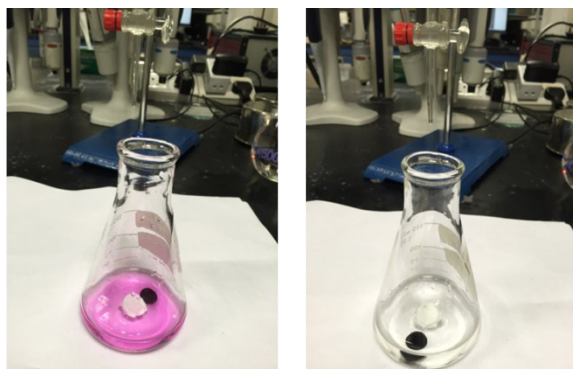


Figure S6. The color changes during the acid-base titration, as well as corresponding equations and ratios of related components.

Table S2. Results of acid-base titration

Samples	HCl Volume (mL)	HCl Mole (μmol)	Li_2O_2 (μmol) (1mAh=18.687 μmol)	Li_2O_2 Yield
Li⁺	6.71	33.55	16.77	89.77%
Na⁺:Li⁺-1:9	6.62	33.10	16.55	88.56%
Na⁺:Li⁺-1:1	6.50	32.50	16.25	86.96%
Na⁺	6.33	31.65	15.83	84.68%

Table S3. DEMS results of gas consumption and evolution during discharging and recharging

Samples	Discharge process			Recharge process			
	Charge passed (μmol)	O ₂ consumed (μmol)	(e^-/O_2)	Charge passed (μmol)	O ₂ evolved (μmol)	CO ₂ evolved (μmol)	(e^-/O_2)
Li ⁺	18.68	9.27	2.01	18.68	7.62	2.60	2.45
Na ⁺ :Li ⁺ -1:1	18.68	9.46	1.97	18.68	6.25	0.15	2.99

During the recharge process, the values of 2.45 and 2.99 e^-/O_2 were obtained for cells with the Li⁺ and Na⁺:Li⁺-1:1 electrolytes respectively, and both values were off ideal 2 e^-/O_2 . This suggested that detrimental parasitic reactions occurred especially for the cell with only Li⁺ electrolyte, accompanied by a high quantity of CO₂ evolved. For the case with the Na⁺:Li⁺-1:1 electrolyte, there could be due to some unclear parasitic reactions. Similar phenomenon was observed by Peng's group,¹⁰ where the H₂O additive can greatly reduce charge polarization and alleviate CO₂ release from parasitic reactions at high potentials, however, the cell's reversibility is slightly destroyed on account of the decreased quantity of O₂ evolved. In spite of this, the above DEMS data on recharge show the recharge ability of the cell with added Na⁺ cation. In this study, our finding demonstrates the beneficial effects of the cation on promoting the formation of defective Li₂O₂ and reducing the charge overpotential on cycling.

Note S2: The different charge profile in Figure 1b and Figure 4d could be due to different discharge and charge conditions. The profile in Figure 1b is conducted at a limited capacity of 1 mAh and a current of 0.1 mA, while the profile in Figure 4d is at a fixed capacity of 0.5 mAh at the current of 1 mA and 0.5 mA for discharge and recharge, respectively.

Note S3: The oxygen evolution rate exceeds the theoretical value of ~2.6 nmol/s in Figure 4b and 4d. This is because that the oxygen evolution rate is not very stable, and sometime much below 2.6 nmol/s.

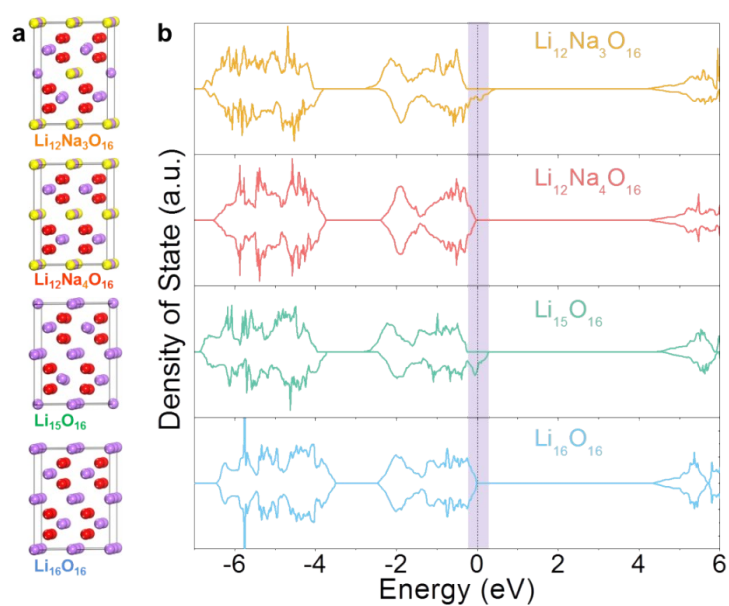


Figure S7. Theoretical simulation results for the proposed Na-doped $\text{Li}_{16}\text{O}_{16}$ structures with three Na ions. **a**, Proposed crystal structure conversion from Li_2O_2 to $\text{Li}_x\text{Na}_y\text{O}_2$. **b**, Corresponding DOS for these proposed structures.

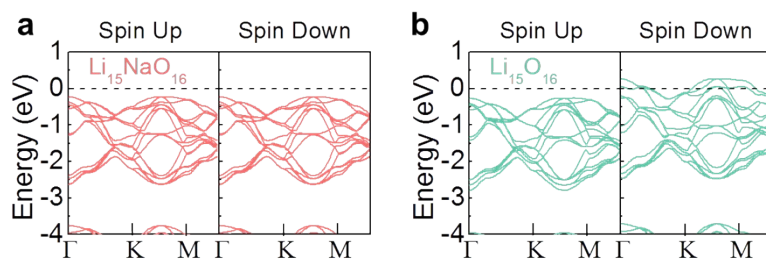


Figure S8. Band structures for $\text{Li}_{15}\text{NaO}_{16}$ (a) and $\text{Li}_{15}\text{O}_{16}$ (b). The horizontal dashed line represents the Fermi level. Spin up and spin down bands are shown in the left and right panels, respectively. Γ , K, and M corresponds three high symmetry points at $(0, 0, 0)$, $(0.5, 0, 0)$, and $(1/3, 1/3, 0)$ in Brouillon zone, respectively.

Table S4. Formation energies of the simulated structures.

	Formation energy (eV / atom)		
	(a)	(b)	(c)
$\text{Li}_{16}\text{O}_{16}$	-1.46	0.00	0.00
$\text{Li}_{15}\text{Na}_1\text{O}_{16}$	-1.42	0.03	0.03
$\text{Li}_{15}\text{O}_{16}$	-1.37	0.05	0.05
$\text{Li}_{14}\text{NaO}_{16}$	-1.34	0.07	0.07
$\text{Li}_{12}\text{Na}_4\text{O}_{16}$	-1.28	0.14	0.16
$\text{Li}_{12}\text{Na}_3\text{O}_{16}$	-1.22	0.17	0.18

(a): energy references are metallic bulk Li and Na

(b): energy references are Li_2O_2 and Na_2O_2

(c): energy references are Li_2O_2 and NaO_2

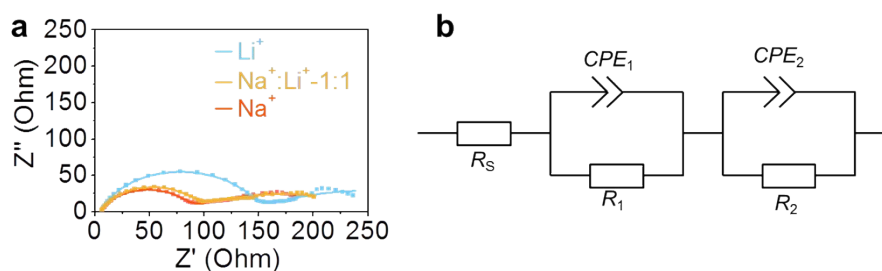


Figure S9. a, Impedance plots for the cells with different marked electrolytes after discharging at a limited capacity of 1 mAh and a current of 0.1 mA. **b**, Schematic of the proposed equivalent circuit, where R and CPE represents resistance and constant phase element, respectively.

Table S5. Resistances from selected impedance fit.

	R_S (Ω)	R_1 (Ω)	R_2 (Ω)	Q_1 ($F s^{n-1}$)	Q_2 ($F s^{n-1}$)	n_1	n_2
Li^+	4.9	217	136	0.01401	7.69E-06	0.33305	0.84526
$Na^+:Li^+-1:1$	4.47	183	80.5	0.007815	1.04E-05	0.33651	0.83034
Na^+	4.82	179	74.2	0.010287	1.20E-05	0.33340	0.81970

Note: Q and n are parameters of the CPE.

As shown in Figure S9, the electrochemical impedance spectra of the cells after discharging were investigated to reveal the reaction kinetics. A proposed equivalent circuit ($R_S(R_1CPE_1)(R_2CPE_2)$) was used to model the impedance plots. Here, R_S represents all the ohmic resistances of cell, and R_1 and R_2 are associated with the charge transfer resistance at the electrolyte/anode interface and the electrolyte/cathode interface, respectively.^{11,12} Clearly, the cells with Na^+ -containing electrolytes ($Na^+:Li^+-1:1$ and Na^+) have smaller charge transfer resistances on the electrolyte/cathode interface after discharge than that with only Li^+ electrolyte, which favor the charging process, thereby leading to a low charge overpotential.

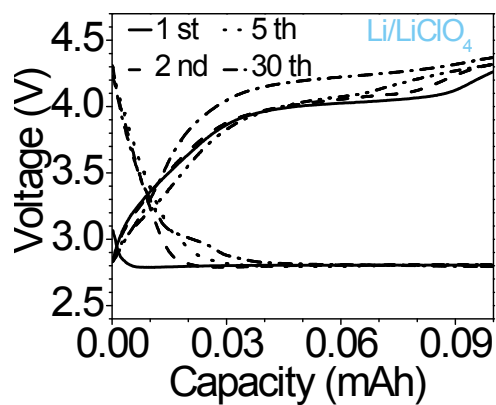


Figure S10. The discharge–charge curves of the cell with LiClO₄ electrolyte at a limited capacity of 0.1 mAh and a current of 0.1 mA.

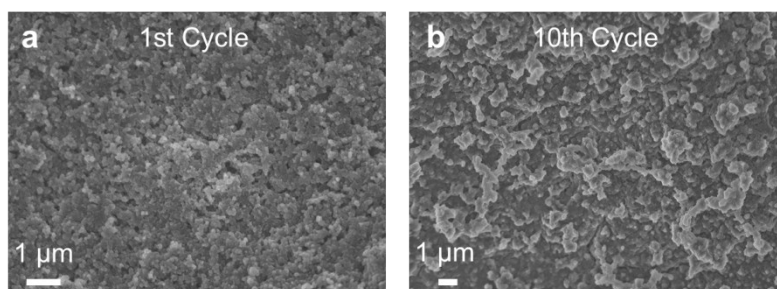


Figure S11. The SEM images for the cathode of the cell with NaClO_4 electrolyte after one and ten cycles at a limited capacity of 0.1 mAh and a current of 0.1 mA.

After 10 cycling, the cathode was passivated by the by-products due to the poor catalytic ability of the pure carbon cathode, which could be one reason for the poor cyclability.

Note S4: The consideration for the reduction of added cations on the unprotected Li anode

Based on the Na^+ concentration of electrolyte (0.25M) and the added amount (50 μL), we can calculate that the amount of Na is as small as ~ 0.25 mg if the added Na^+ is fully reduced on the anode. Such small amount of Na cannot be uniformly deposited, and hence the surface of Li anode after charging is almost Li. Moreover, we observed that the surface of the cycled Li anode looked fresh after disassembly, and XPS characterization indicated negligible Na signal on the Li anode after first discharge-charge cycle (Fig. S12).

In addition, although the cation could be reduced on the anode, such small amount of the deposited cations can also be oxidized and diffuse into the electrolyte during the next discharging process. This concern regarding unexpected reactions of Na^+ with Li metal anode can be excluded by the use of ceramic Li ion conductor.

In this study, we propose a demonstration to form the defective Li_2O_2 that can reduce the charge overpotential of the Li- O_2 batteries. We believe that the cycle performance of the batteries with added cations can be greatly enhanced when the selective separator is developed or the protection technology of lithium anode is maturity. Moreover, the protection of the lithium anode is obligatory for Li-metal anode batteries, considering the safety and cycle ability. Currently consider research works are devoted to developing advanced Li anode. In the Li- O_2 batteries system, the corrosion of lithium anode is common and serious problem for any organic liquid electrolytes. Especially, the oxygen crossover from the cathode to the anode is well-known to result in oxidation of the lithium anode and to limit cycle life.

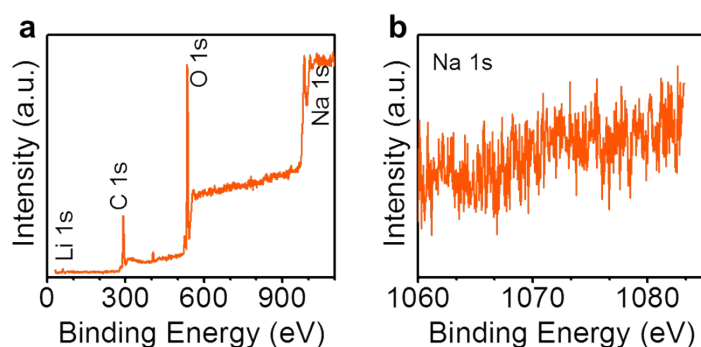


Figure S12. XPS characterizations of the Li anode after first discharge-charge cycle for the cell with the $\text{Na}^+:\text{Li}^+ - 1:1$ electrolyte.

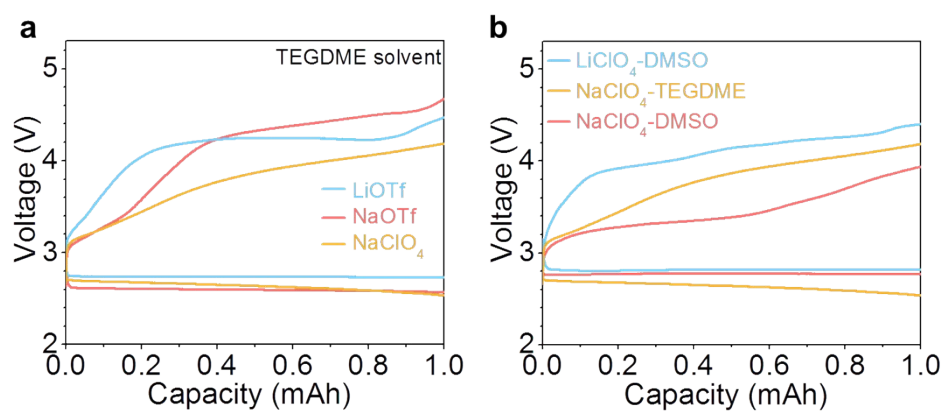


Figure S13. Effects of Na⁺ cation and TEGDME solvent on the charge performances at a limited capacity of 1 mAh and a current of 0.1 mA. **a**, The effect of the added Na⁺ cation in TEGDME solvent. **b**, The effect of the TEGDME solvent.

References

1. Kresse, G.; Furthmüller, J. Efficiency of Ab-initio Total Energy Calculations for Metals and Semiconductors Using a Plane-Wave Basis Set. *Comput. Mater. Sci.* **6**, 15-50 (1996).
2. Kresse, G.; Furthmüller, J. Efficient Iterative Schemes for Ab initio Total-Energy Calculations Using a Plane-Wave Basis Set. *Phys. Rev. B* **54**, 11169-11186 (1996).
3. Blochl, P. E. Projector Augmented-Wave Method. *Phys. Rev. B* **50**, 17953-17979 (1994).
4. Kresse, G. From Ultrasoft Pseudopotentials to the Projector Augmented-Wave Method. *Phys. Rev. B* **59**, 1758-1775 (1999).
5. Heyd, J.; Scuseria, G. E.; Ernzerhof, M. *J. Chem. Phys.* **118**, 8207 (2003).
6. Paier, J.; Marsman, M.; Hummer, K.; Kresse, G.; Gerber, I. C.; Angyan, J. G. *J. Chem. Phys.* **125**, 249901 (2006).
7. Methfessel, M.; Paxton, A. T.; High-Precision Sampling for Brillouin-zone Integration in Metals. *Phys. Rev. B* **40**, 3616-3621 (1989).
8. Foppl, H.; *Anorg. Z. Allg. Chem.* **291**, 12 (1957).
9. Gao, X.; Chen, Y.; Johnson, L.; Bruce, P. G. Promoting solution phase discharge in Li-O₂ batteries containing weakly solvating electrolyte solutions. *Nat. Mater.* **15**, 882–888 (2016).
10. Ma, S., Wang, J., Huang, J., Zhou, Z. & Peng, Z. Unveiling the Complex Effects of H₂O on Discharge–Recharge Behaviors of Aprotic Lithium–O₂ Batteries. *J. Phy. Chem. Lett.* **9**, 3333-3339 (2018).
11. Højberg, J.; McCloskey, B. D.; Hjelm, J.; Vegge, T.; Johansen, K.; Norby, P.; Luntz, A. C., An Electrochemical Impedance Spectroscopy Investigation of the Overpotentials in Li-O₂ Batteries. *ACS Appl. Mater. Interfaces* **7**, 4039-4047 (2015).
12. Landa-Medrano, I.; Ruiz de Larramendi, I.; Ortiz-Vitoriano, N.; Pinedo, R.; Ignacio Ruiz de Larramendi, J.; Rojo, T., In situ monitoring of discharge/charge processes in Li–O₂ batteries by electrochemical impedance spectroscopy. *J. Power Sources* **249**, 110-117 (2014).